SEBBM 2021

43rd Annual Meeting of the Spanish Society of Biochemistry & Molecular Biology

BARCELONA 19-22 JULY

BOOK OF ABSTRACTS

v.2

ORGANIZES:

SEBBM

Currently, given the scarcity of generated RPR tests, the implementation of the reverse algorithm has proved to be an asset in the automation and optimization of other laboratory processes through a better human resource management. In addition, there is a moderate prevalence of HIV and other risk factors for syphilis in this region, which cannot be undervalued, increasing the likelihood of syphilis, which are not so well diagnosed by non-treponemal methods. Therefore, the implementation of this algorithm has consolidated its added value.

1.The laboratory diagnosis of syphilis.2005 2.Laboratory Diagnostic Tools for Syphilis:Current Status and Future Prospects.2021 3.The Traditional or Reverse Algorithm for Diagnosis of Syphilis:Pros and Cons.2020 4.Screening for syphilis with the treponemal immunoassay: analysis of discordant serology results and implications for clinical management.2011. 5.It is time to use treponema-specific antibody screening tests for diagnosis of syphilis.2012

0420-P

Cytolocalyzation and cytotoxicity of new luminescent cyclometalated platinum(II) complexes: use as organelle biomarkers and antitumoral drugs with potential in photodynamic therapy

JOSÉ G. PICHEL [1], REBECA LARA [2], MÓNICA MARTÍNEZ-JUNQUERA [3], GONZALO MILLÁN [3], ELVIRA ALFARO-ARNEDO [3], M. TERESA MORENO [2], IGNACIO M. LARRÁYOZ [2], ICÍAR P. LÓPEZ [2], ELENA LALINDE [2]

[1]Fundación Rioja Salud (CIBIR), Logroño & CIBERES, ISCIII. Lung Cancer and Respiratory Diseases Unit, [2]Universidad de La Rioja, Logroño Departamento de Química-Centro de Síntesis Química de La Rioja, (CISQ), [3]Departamento de Química-Centro de Síntesis Química de La Rioja, (CISQ) Departamento de Química-Centro de Síntesis Química de La Rioja, (CISQ)

Two series of luminescent cyclometalated Pt(II) complexes were synthesized a nd their biological activity was assessed. One was based on the deprotonated donor-acceptor 2-(4-dimethylaminephenyl)benzothiazole ligand (**NMe_2-pbt**) and includes four mononuclear complexes [Pt(Me_2N-pbt)(C_6F_5)L] (L = Me_2N-pbtH) **1**, *p*-dpbH (4-diphenylphosphino)benzoic acid) **2**, *o*-dpbH (2-diphenylphosphino)benzoic acid) [Pt(Me_2N-pbt)(C_6F_5)(*o*-dpbH)] **3** (unstable), and [Pt(Me_2N-pbt)(*o*-dpb)] **4**, as well as of two binuclear derivatives [{Pt(Me_2N-pbt)(C_6F_5)}2(m-PR_nP)] [PR_4P = O($CH_2CH_2OC(O)C_6H_4PPh_2$)2 **5**; $PR_{12}P$ = O{(CH_2CH_2O)3C(O)$C_6H_4PPh_2$}2 **6**]. The second includes 2,6-difluorophenylpyridine (dfppy) and phenylquinoline (pq) as chromophores and acyclic diaminocarbene (ADC) ligands as auxiliary ligands [Pt(C^N)Cl{C(NHXyl)(NHR)}] [C^N = dfppy (**a**), pq (**b**); R = Pr **7a**, **8a**, CH_2Ph **7b**, **8b**]. In the NMe_2-pbt based complexes the phosphorescent emission is lost in aerated solutions, owing to photoinduced electron transfer to $^3O_2$ and formation $^1O_2$ singlet, as confirmed in complexes **2** and **4**. Here we report some of their biological activity. Cytotoxicity studies in the human cancer cell lines A549 (lung carcinoma) and HeLa (cervix carcinoma) showed good activity for the ADC complexes **7** and **8**. To the best of our knowledge, these compounds represent the first examples of cycloplatinated complexes bearing acyclic diamino carbenes with antiproliferative properties (Ref.). Accordingly, **7a**, **7b** and **8a** altered DNA electrophoretic mobility pointing as a possible cytotoxic mechanism. NMe_2-pbt complexes **2**, **3** and **6** were also active against A549 and HeLa cancer cells, with higher efficiency in A549, in contrast to **1**, **4**, and **5**. Cytolocalization studies revealed that the no cytotoxic ligand **Me_2N-pbtH** and their derivative complexes **1-6** exhibit specific accumulation in the Golgi apparatus. Furthermore, the potential photodynamic property of this type of complexes was demonstrated with the non-cytotoxic complex **4**, which demonstrated efficient photoinduced cytotoxicity after irradiation.

Funding: ADER La Rioja Project 2017-I-IDD-0031 and MICINN Project PID2019-109742GB-I00, both co-founded by the European Regional Development and European Social Funds (ERDF/ESF). RL, MM-J and GM, and E.A-A PhD fellowships are granted by Univ. La Rioja and the Spanish Association Against Cancer (AECC), respectively.

0454-P

A chemical tool to unravel HIV-1 palmitoylome

AROA ARBOLEYA [1], JON ANDER NIETO-GARAI [2], F.-XABIER CONTRERAS [2], MAIER LORIZATE [2]

[1]Instituto Biofísika - Universidad del País Vasco Biochemistry and Molecular Biology, [2]Instituto Biofísika - Universidad del País Vasco Biochemistry and Molecular Biology

The major function of palmitoylation is to mediate stable membrane attachment of soluble proteins. There are multiple viral palmitoylated proteins. One of the most known is the envelope glycoprotein of HIV-1 virus, which is embedded within the viral membrane. It allows the virus to attach and fuse to target cells, starting the infectious cycle. It is composed by two subunits: the transmembrane subunit gp41 and the surface subunit gp120. Gp41 is palmitoylated in four highly conserved cysteine residues: Cys-598, Cys-604, Cys-764 and Cys-837. Cys-764 and Cys-837 are located in the Lentiviral Lytic Peptides (LLPs) of the cytoplasmic tail. Palmitate groups covalently attached to these cysteines insert into the lipid bilayer, interacting with different membrane proteins during HIV-1 budding and assembly, and anchor gp41 to the cell membrane. Furthermore, HIV-1 virions contain cellular membrane proteins, which are caught during budding from cellular membranes. Nowadays, HIV-1 proteome is described, however, a detailed HIV-1 palmitoylome remains undiscovered.

An alkyne-modified palmitoyl compound was synthetized,

Gobierno de La Rioja
www.larioja.org

Rioja Salud

43 Congreso de la SEBBM
Barcelona, 19-22 July 2021

Cytolocalyzation and cytotoxicity of new luminescent cyclometalated platinum(II) complexes: use as organelle biomarkers and antitumoral drugs with potential in photodynamic therapy

José G. Pichel[a,b], Rebeca Lara[c], Mónica Martínez-Junquera[c], Gonzalo Millán[c], Elvira Alfaro-Arnedo[a], M. Teresa Moreno[c], Ignacio M. Larráyoz[d], Icíar P. López[a] and Elena Lalinde[c]

[a]*Lung Cancer and Respiratory Diseases Unit (CIBIR), *Fundación Rioja Salud (FRS). Logroño;* [b]Biomedical Research Networking Center in Respiratory Diseases (CIBERES), ISCIII; [c]Departamento de Química-Centro de Síntesis Química de La Rioja, (CISQ), Universidad de La Rioja. Logroño; [d]Biomarkers and Molecular Signaling Unit (CIBIR), FRS. Logroño.

CIBIR Centro de Investigación Biomédica de La Rioja

UNIVERSIDAD DE LA RIOJA
Logroño, SPAIN

P 420

INTRODUCTION

Among phosphorescent molecules, cyclometalated platinum(II) complexes have received attention because of their photophysical properties and potential applications as dopants in OLEDs, LECs, photocatalysts or bioimaging. Another research of relevant interest is their employment as anticancer drugs with a broader spectrum of action against different tumours and fewer side effects than the well-known cisplatin. For that reason, the choice of the cyclometalated group and ancillary ligands play an important role not only in emissive behavior but also on the biological activity (1).

Benzothiazole show a wide range of applicability in medicinal chemistry. In particular, 2-arylbenzothiazoles have demonstrated potent antitumor activity (2-3). In particular, 2-(4-dimethylaminophenyl)benzothiazole (**Me$_2$N-pbtH**), a simple molecule with donor-acceptor properties, has been extensively studied due to its interesting photophysical properties (4). However, reports related to biological activity of cyclometalated complexes based on this ligand are extremely limited (5). Our group recently reported on the synthesis and intriguing photophysical properties of several [Pt(Me$_2$N-pbt)ClL] [L = DMSO; 1,3,5-triaza-7-phosphaadamantane (PTA); 3,3,3''-trisulfonate sodium salt (TPPTS)] that revealed perinuclear staining and moderate cytotoxic activity for the DMSO and PTA complexes towards the human cell lines A549 and HeLa, which was suggested to be governed by inhibition of tubulin polymerization (5). Similar perinuclear localization with improved bioactivity was observed in pentafluorophenyl-cyclopalitated complexes [Pt(C^N)(C$_6$F$_5$)L] (C^N = ppy, dfppy) incorporating DMSO and the biocompatible phosphine 4-(diphenylphosphino)benzoic acid (PPh$_2$C$_6$H$_4$COOH, dpbH) as auxiliary ligands (6).

To further investigate the biological properties of new cyclometalated Pt(II) complexes featuring the **Me2N-pbt** scaffold and incorporating non leaving carboxy-substituted phosphine ligands were synthesized and analyzed. Here, we present the biological activity of new mononuclear complexes [Pt(Me$_2$N-pbt)(C$_6$F$_5$)L] (L = Me$_2$N-pbtH **1**, p-dpbH **2**, o-dpbH **3**) and [Pt(Me$_2$N-pbt)(o-dpb)] **4**. For comparative purposes,, we also present two binuclear complexes [{Pt(Me$_2$N-pbt)(C$_6$F$_5$)}$_2$(μ-PR$_2$P)] [PR$_2$P = *O*(CH$_2$CH$_2$OC(*O*)C$_6$H$_4$PPh$_2$)$_2$ **5**; PR$_2$P = *O*{(CH$_2$CH$_2$O)$_2$C(*O*)C$_6$H$_4$PPh$_2$}$_2$ **6**], with the Pt units connected by a diphosphine having two distinct ethylene glycol units. Complexes **1-6** display 1ILCT and metal perturbed 3ILCT dual emissions. The ratio between both bands is excitation dependent, accomplishing warm-white emissions for **2**, **5** and **6** and the triplet emission is lost in aerated solutions, owing to photoinduced electron transfer to $^3O_2$ and formation of $^1O_2$. They also exhibit photoinduced phosphorescence enhancement in non-degassed DMSO, due to local oxidation of DMSO by sensitized $^1O_2$, which remove $^3O_2$.

On the other hand, N-acyclic diaminocarbenes (ADCs) also show several appealing characteristics; they display strong electron-donating ability with structural flexibility and can be easily prepared. However, there are only a few examples of ADC-platinum complexes used as perspective metal-based drugs in the literature (7). Thus, here we also present the biological properties of a series of new luminescent ADC cycloplatinated(II) compounds featuring 2-(2,4-difluorophenyl)pyridine (**7**) and 2-phenylquinoline (**8**) cyclometalated groups [Pt(C^N)Cl{C(NHXyl)(NHR)}] (R = Pr **a**, Benzyl **b**) obtained by nucleophilic addition of primary propyl and benzyl amines, to the isocyanide ligand of the corresponding precursors [Pt(C^N)Cl(CNXyl)] (**1**, **2**) recently reported by our group (8,9). These complexes show green (**7**) or orange (**8**) phosphorescence,attributed to a mixed 3IL/3MLCT excited state. The carbene ligand does not affect the emission maxima but it produces an increase of the quantum yields in relation to the isocyanide in the precursors. In fluid solutions, the emission is not concentration-dependent, but the complexes may show aggregation induced emission as detailed for complexes **7a** and **8a** (9).

RESULTS

1 Synthesis of complexes **1-6**, emission spectra and energy levels of singlet and triplet states. Excitation and emission of **2** in DMSO in the presence of O_2

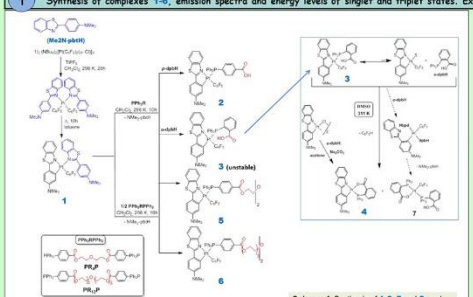

Scheme 1. Synthesis of **1-3**, **5** and **6**, and evolution of **3** to **4** in DMSO at 311 K (Heat).

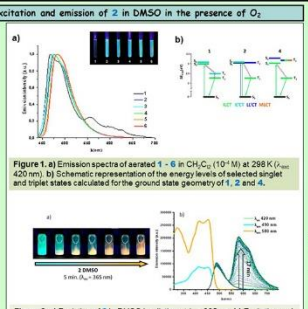

Figure 2. a) Evolution of 2 in DMSO irradiating at λex 365 nm. b) Excitation and emission of 2 in DMSO 10^{-5} M in the presence of O_2 with different irradiation times

Figure 1. a) Emission spectra of aerated **1 - 6** in CH_2Cl_2 (10^{-5} M) at 298 K (λ_{exc} 420 nm). b) Schematic representation of the energy levels of selected singlet and triplet states calculated for the ground state geometry of **1**, **2** and **4**.

2 While complexes **Me2N-pbtH**, **1** and **5** were non-toxic, **2**, **3** and **6** showed similar citotoxity than **cisplatin** towards tumor cell lines. Non-toxic **4** exhibit hight antitumor activity upon UV irradiation as a photosensitizer for the generation of singlet $^1O_2$

Table 1. Cytotoxic IC_{50} values (μM)* of the **NMe$_2$-pbt** ligand, derivatives Pt(II)-complexes **1-6** and cisplatin towards A549 (lung adenocarcinoma) y HeLa (cervix carcinoma) human tumor cell lines.

Compound	A549*	HeLa*
NMe$_2$-Hpbt	NT	-
1 [Pt(Me$_2$N-pbt-κC,N)(Me$_2$N Hpbt-κN)(C$_6$F$_5$)]	NT	-
2 [Pt(Me$_2$N-pbt-κC,N)(C$_6$F$_5$)(o-dpbH)]	8.39 ± 0.75	30.82 ± 1.05
3 [Pt(Me$_2$N-pbt-κC,N)(C$_6$F$_5$)(o-dpbH)]	11.59 ± 1.40	16.51 ± 0.57
4 [Pt(Me$_2$N-pbt-κC,N)(o-dpb-κP,O)]	NT	-
5 [{Pt(Me$_2$N-pbt-κC,N)(C$_6$F$_5$)}$_2$(μ-PR$_2$P)]	NT*	-
6 [{Pt(Me$_2$N-pbt-κC,N)(C$_6$F$_5$)}$_2$(μ-PR$_2$P)]	10.48 ± 0.05	48.25 ± 1.23
Cisplatin	6.45 ± 0.47	13.60 ± 0.99

*IC_{50} values (μM) are presented as mean ± the standard error of the mean of three different experiments performed in sextuplicates. IC_{50} values were determined by MTT assays after cellular exposure to the compounds for 72 h. *No soluble in cell culture medium. NT, non toxic

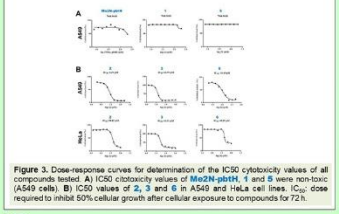

Figure 3. Dose-response curves for determination of the IC50 cytotoxicity values of all compounds tested. **A)** IC50 citotoxicity values of **Me2N-pbtH**, **1** and **5** were non-toxic (A549 cells). **B)** IC50 values of **2**, **3** and **6** in A549 and HeLa cell lines. IC_{50}: dose required to inhibit 50% cellular growth after cellular exposure to compounds for 72 h.

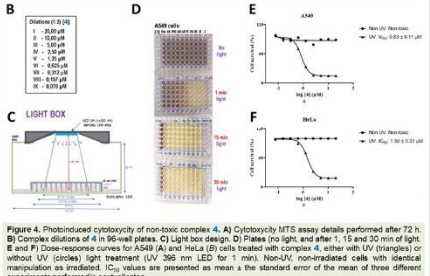

Figure 4. Photoinduced cytotoxicity of non-toxic complex **4**. **A)** Cytotoxicity MTS assay details performed after 72 h. **B)** Complex dilutions of **4** in 96-well plates. **C)** Light box design. **D)** Plates (no light, and after 1, 15 and 30 min of light. **E** and **F)** Dose-response curves for A549 (A) and HeLa (B) cells treated with complex **4**, either with UV (triangles) or without UV (circles) light treatment (UV 395 nm LED for 1 min). Non-UV, non-irradiated cells with identical manipulation as irradiated. IC_{50} values are presented as mean ± the standard error of the mean of three different experiments performed in sextuplicates.

3 **1**, **2** and **6** do not interact with pBR322 DNA as **cisplatin** does; and **2** and **6** do not depolimerize microtubules as nocodazole does.

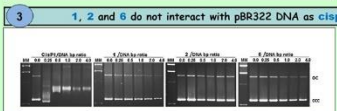

Figure 5. Electrophoresis mobility shift assay for **cisplatin** and compounds **1**, **2** and **6**. CisPt: cisplatin; **MM**, λHindIII DNA molecular marker; Numbers refer to complex/plasmid DNA (pBR322); base pairs (bp) increasing ratios; **OC**, open circular (relaxed) plasmid DNA form; **CCC**, covalently closed circular (supercoiled) plasmid DNA form.

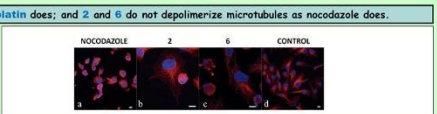

Figure 6. Laser scanning confocal microscopy images of fixed A549 cells treated with **a)** 100 μM nocodazole (microtubule targeting agent) for 2 h, **b)** **100 μM** compound **2** for 6 h, **c)** **100 μM** compound **6** for 6 h or **d)** control cells. Red: **tubulin** antibody staining (λex 543 nm); Blue: nuclei marker (**DAPI**, λex 405 nm). CONTROL, non-treated cells (bar = 10 μm).

4 Time-course of cytosolic accumulation of **Me2N-pbtH**, **1**, **2**, **4** and **6** and partial co-localization in lysosomes, but not in mitochondria

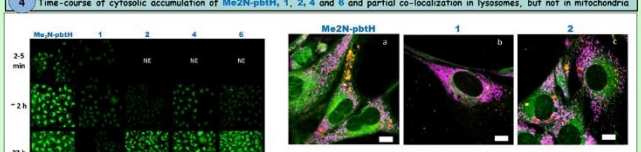

Figure 7. Laser scanning confocal microscopy images of live A549 cells incubated with 10 μM **Me2N-pbtH** (ligand), **1**, **2**, **4** or **6** (green) for the indicated times (λex 405 nm. NE: non emissive).

Figure 8. Laser scanning confocal microscopy images of live **LMEF cells** incubated with 10 μM **Me2N-pbtH** **a)**, **1** b) or **2** c), during 22 h and simultaneous co-staining with LysoTracker and MitoTracker. Green: Ligand/compound (λex 405 nm); Red: **LysoTracker** (**Lysosomal marker**, λex 543 nm); Magenta: **MitoTracker** (**Mitochondrial marker**, λex 633 nm). Yellow colour indicates colocalization between ligand or compounds (green) and LysoTracker (red). There is no evidence of co-localization of ligand or compound with MitoTracker (bar = 10 μm).

5 **NMe$_2$-Hpbt** and **2** are good **Golgi apparatus** biomarkers:
Most of their phosphorescent signal colocalize with **BODIPY TR C5 Ceramide**, a Golgi marker

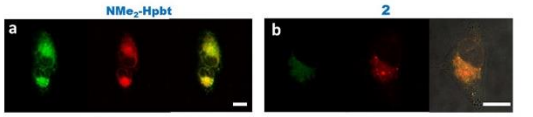

Figure 9. Laser scanning confocal microscopy images of live A549 cells incubated with **a)** 10 μM **Me2N-pbtH** (ligand) for 2 h, or **b)** 10 μM **2** during 4 h (signal in green, left panels), in the presence of **BODIPY TR C5 Ceramide** (**Golgi apparatus marker**) (signal in red, central panels). **Green: Ligand/compound** (λex 405 nm); **Red: BODIPY TR C5** Ceramide (Golgi apparatus marker, λex 543 nm). Superimposed images are shown in the right panels, where yellow/orange colours indicate colocalization between ligand/compound (green) and BODIPY TR C5 Ceramide (red) in the Golgi apparatus (bar = 10 μm).

6 Synthesis and emission spectra of N-acyclic diaminocarbenes complexes **7a**, **7b**, **8a** and **8b**.

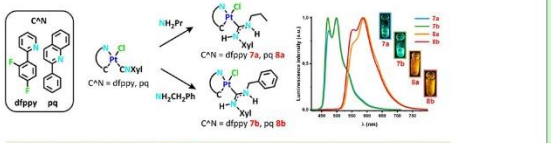

Figure 10. Scheme of the synthesis of **7a**, **7b**, **8a** and **8b** and selected emission spectra of all compounds in 5% PS (9).

7 **7a**, **7b**, **8a** and **8b** complexes display higher in vitro cytotoxicity than cisplatin toward the A549 and HeLa cell lines.

Table 2. Cytotoxic IC_{50} values (μM)* of the complexes **7a**, **7b**, **8a**, **8b** and cisplatin in human cancer cell lines A549 (lung adenocarcinoma) y HeLa (cervix carcinoma)

Compound	A549*	HeLa*
7a	11.85 ± 2.02	8.88 ± 2.02
7b	8.81 ± 0.88	7.31 ± 0.95
8a	8.52 ± 0.58	10.02 ± 1.59
8b	4.74 ± 0.49	4.44 ± 0.89
Cisplatin	6.45 ± 0.47	13.60 ± 0.99

*IC_{50} values (μM) are presented as mean ± the standard error of the mean of three different experiments performed in sextuplicates. IC_{50} values were determined by MTT assays after cellular exposure to the compounds for 72 h.

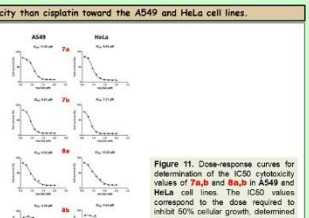

Figure 11. Dose-response curves for determination of the IC50 cytotoxicity values of **7a,b** and **8a,b** in **A549** and **HeLa** cell lines. The IC50 values correspond to the dose required to inhibit 50% cellular growth, determined from the dose-dependence of surviving cells after cellular exposure to compounds for 72 h.

8 **7a**, **7b**, and **8a** . 7a, 7b and 8a exhibit an effect on DNA electrophoretic mobility which differs from that of cisplatin.

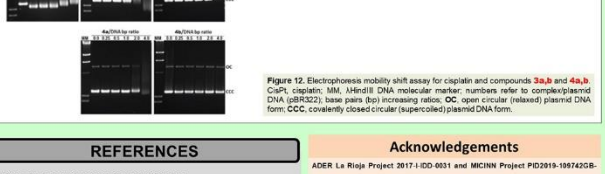

Figure 12. Electrophoresis mobility shift assay for cisplatin and compounds **3a,b** and **4a,b** CisPt: cisplatin; MM, λHindIII DNA molecular marker; numbers refer to complex/plasmid DNA (pBR322); base pairs (bp) increasing ratios; **OC**, open circular (relaxed) plasmid DNA form; **CCC**, covalently closed circular (supercoiled) plasmid DNA form.

CONCLUSIONS

1. Mono and binuclear cycloplatinated complexes (**1 - 6**) featuring the donor-acceptor 2-(4-dimethylaminophenyl)benzothiazolyl ligand (**NMe2-pbt**) and biologically active phosphines show dual emission and photoinduced phosphorescence generating $^1O_2$, with potential applications in theranostics and photodynamic therapy.

2. N-acyclic diaminocarbenes complexes **7a**, **7b**, **8a** and **8b** complexes display higher *in vitro* cytotoxicity than cisplatin toward the A549 and HeLa cell lines. Complexes **7a**, **7b** and **8a** exhibit an effect on DNA electrophoretic mobility which differs from that of cisplatin. The present work suggests that cyclometalated Pt(II)-ADC complexes may have applications as highly effective anticancer drugs.

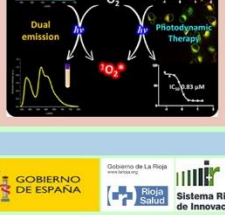

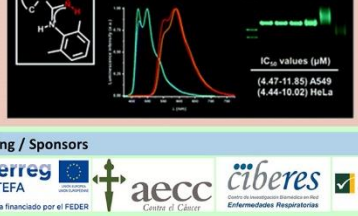

REFERENCES

1. P. Zhang, P.J. Sadler. ***J. Organomet. Chem.*, 2017, 839,** 5-14.
2. L. Hroch, L. Aitken, O. Benek, M. Dolezal, K. Kuca, F. Gunn-Moore, K. **Musilek.** ***Curr. Med. Chem.* 2015, 22,** 730-747.
3. ***A.K. Sharma, J.W. Schultz, J.T. Prior, N. P. Rath, L.M. Mirica, Inorg. Chem.* 2017, 56,** 13801-13804.
4. F. Hualong, C. Mengchao. ***Curr. Med. Chem.* 2018, 25,** 2736-2759.
5. E. Lalinde, M.T. Moreno, R. Lara, I.P. López, E. Alfaro-Arnedo, J.G. Pichel, S. Piñeiro-Hermida. ***Chem. Eur. J.* 2018, 24, 2440-2456.**
6. G. Millán, N. Giménez, R. Lara, J.R. Berenguer, M.T. Moreno, E. Lalinde, E. Alfaro-Arnedo, I.P. López, S. Piñeiro-Hermida, J.G. Pichel. ***Inorg. Chem.* 2019, 58,** 1657-1673.
7. I.V. Seredyanskaya, M. A. Kinzhalov, et al., ***New J. Chem.*, 2020, 44,** 5762-5773.
8. M. Martínez-Junquera, R. Lara, E. Lalinde, M.T. Moreno. ***J. Mater. Chem. C*, 2020, 8,** 7221-7233.
9. M. Martínez-Junquera, E. Lalinde, M.T. Moreno, E. Alfaro-Arnedo, I.P. López, I.M. Larráyoz and J.G. Pichel ***Dalton Trans*, 2021, 50,** 4539-4554.

Acknowledgements

ADER La Rioja Project 2017-I-IDD-0031 and MICINN Project PID2019-106742GB-I00, both co-founded by the European Regional Development and European Social Funds (ERDF/ESF). RL, MM-J and GM, and E.A-A PhD fellowships are granted by Univ. La Rioja and the Spanish Association Against Cancer (AECC), respectively.

Funding / Sponsors

GOBIERNO DE ESPAÑA
Gobierno de La Rioja
Rioja Salud
Sistema Riojano de Innovación
Interreg POCTEFA
Programa financiado por el FEDER
aecc Contra el Cáncer
ciberes Centro de Investigación Biomédica en Red Enfermedades Respiratorias
Gobierno de La Rioja
ader Agencia de Desarrollo Económico de La Rioja